Sediment Acoustics: Wideband Model, Reflection Loss and Ambient Noise Inversion

Nicholas P. Chotiros
Applied Research Laboratories
The University of Texas
Austin, TX 78713-8029
phone: (512) 835-3512 fax: (512) 835-3259 email: chotiros@arlut.utexas.edu

Award Number: N00014-06-1-0125
http://www.arlut.utexas.edu/

LONG-TERM GOALS

Physically sound models of acoustic interaction with the ocean floor including penetration, reflection and scattering in support of MCM and ASW needs.

OBJECTIVES

(1) Consolidation of the BIC08 model of sediment acoustics, its verification in a variety of sediment types, parameter reduction and documentation in preparation for transition. (2) A new model of sediment reflection based on a mixture of models suitable for shallow water sonars. (3) Coupling of BIC08 to rough surface scattering models.

APPROACH

(1) Consolidation of the BIC08 model: This model contains plausible physical processes. It is based on the **Bi**ot-Stoll grain **c**ontact **sq**uirt flow and **s**hear viscous drag (BICSQS) model, which includes squirt flow at the grain-grain contacts [Chotiros, Isakson 2004], combined with improvements in squirt flow modeling, the frame virtual mass extension to account for the random grains rotation [Chotiros, Isakson 2007], and the high-frequency viscous drag correction [Chotiros, Isakson 2008]. The approach is to reconcile common parameters in the different components, and consolidate the input parameters to reduce the parameter count. In the process of doing so, it was found necessary to invoke micro-fluidic viscosity enhancements [Goertz et al. 2007, Riedo 2007]. This lead to a reduction in the number of input parameters, which is important for making the model usable in practical applications. The latest model is designated BIC11.

(2) A new model of sediment reflection: This is a new approach to modeling ocean sediments that recognizes that the sediment is often patchy. The reflection measurements from the SAX04 experiment [Isakson, Chotiros, Camin, Piper 2010] are an extreme example. It suggests a new approach to modeling bottom reflection as a random process, in which each bottom bounce contains both a deterministic as well as a random component. This approach is consistent with recent findings that bottom backscatter is often well described by a mixture of processes [Lyons and Abraham 1999], and

Report Documentation Page

Form Approved
OMB No. 0704-0188

1. REPORT DATE	2. REPORT TYPE	3. DATES COVERED
SEP 2011		**00-00-2011 to 00-00-2011**

4. TITLE AND SUBTITLE	5a. CONTRACT NUMBER
Sediment Acoustics: Wideband Model, Reflection Loss and Ambient Noise Inversion	5b. GRANT NUMBER
	5c. PROGRAM ELEMENT NUMBER
6. AUTHOR(S)	5d. PROJECT NUMBER
	5e. TASK NUMBER
	5f. WORK UNIT NUMBER
7. PERFORMING ORGANIZATION NAME(S) AND ADDRESS(ES) **University of Texas,Applied Research Laboratories,Austin,TX,78713-8029**	8. PERFORMING ORGANIZATION REPORT NUMBER
9. SPONSORING/MONITORING AGENCY NAME(S) AND ADDRESS(ES)	10. SPONSOR/MONITOR'S ACRONYM(S)
	11. SPONSOR/MONITOR'S REPORT NUMBER(S)

12. DISTRIBUTION/AVAILABILITY STATEMENT
Approved for public release; distribution unlimited

13. SUPPLEMENTARY NOTES

14. ABSTRACT

15. SUBJECT TERMS

16. SECURITY CLASSIFICATION OF:			17. LIMITATION OF ABSTRACT	18. NUMBER OF PAGES	19a. NAME OF RESPONSIBLE PERSON
a. REPORT	b. ABSTRACT	c. THIS PAGE			
unclassified	**unclassified**	**unclassified**	**Same as Report (SAR)**	**13**	

with analyses of transmission loss (TL) inversion of data collected by NAVO. It will lead to more realistic bottom models for sonar performance prediction.

(3) Coupling of BIC08 to rough surface scattering models: Since the real ocean bottom is rough, it is necessary to be able to combine the elastic and/or poro-elastic models, such as BIC08, with a rough interface, in order to obtain a realistic model of the bottom. For a computationally fast solution, a ray-based approach is likely to be a practical solution, but for accuracy, a finite element model (FEM) approach is needed. This task also includes experimental support equipment to measure seafloor roughness, to allow rough interface scattering models to be tested with at-sea experimental measurements.

WORK COMPLETED

Following the three tasks mentioned in the approach, the work completed may be divided into three corresponding sections:

(1) Consolidation of the BIC08 model: There are at least two issues to resolve in order to move forward. One is an accurate expression of shear wave speed in a granular medium, and it is closely connected with the low-frequency sound speed anomaly. Another is the reconciliation of parameter values that are used in different components of the model, and the alignment of the physical submodels.

It was established that the shear wave speed in a granular medium is less than that in an elastic solid of the same shear modulus-to-density ratio. Shear and compressional wave speeds were derived for granular media using a conservation of energy approach. The grains were assumed to be spherical with elastic Hertzian contacts of constant stiffness. Invoking the affine and effective medium approximations, it was found that shear wave propagation in a granular medium involves additional energies associated with grain rotation. The partition of energies results in a reduction in the shear wave speed, relative to an elastic solid of the same shear modulus-to-density ratio. The predicted wave speed ratios are consistent with published measurements [Chotiros and Isakson 2011].

This work is being extended to model the effects of variable contact stiffness, and it is expected to shed some light on the low-frequency sound speed anomaly, in which the sound speed in granular sediments is often found to be lower than the Wood's equation lower bound. It was also found that the squirt flow component of BIC08 was giving unphysical values for the fluid film at the grain-grain contacts. This issue was resolved by taking account of the increase in viscosity, for nanometer-scale interfacial separations [Goertz, Houston, and Zhu 2007]. This work has produced a reduction in the number of input parameter, and the improved model is designated BIC11.

(2) A new model of sediment reflection: Transmission loss (TL) data provided by NAVO were revisited and the results indicate seabed variability or patchiness, particularly for the higher frequencies. The heterogeneity is on a scale that is too fine to be properly mapped and may change as a function of time, and therefore it has to be treated statistically. In this approach, the key parameters include the amplitude and the spatial correlation function of the fluctuations.

(3) Coupling of BIC08 to rough surface scattering models: There were some practical issues to be resolved, regarding the spatial sampling of the medium for finite element modeling (FEM). In sandy sediments, the Biot slow wave and the shear wave, which are predicted to have low wave speeds, require very dense meshing of the medium model. A similar problem exists with elastic media with low shear wave speeds. The problem was studied in the context of propagation in a shallow water waveguide over an elastic half space seabed. The elastic half space was approximated by a thin layer of elastic medium over a fluid half space with the same density and sound speed. Tests showed that the approach may be feasible.

RESULTS

The results are presented in the same order as the work completed:

(1) Progress in consolidation of the BIC08 model:

A key issue is an accurate expression for wave speeds in a granular medium. The new granular medium model [Chotiros and Isakson 2011] solved the inconsistency in the shear wave speed for granular media. Building upon this foundation, the model is being extended to a more realistic granular media, in which the grain contact stiffness is variable. This topic has been studied by other researchers using numerical models with some success [Jenkins, Johnson, Ragione, and Makse 2005, Ragione and Jenkins 2007] , but their models are complicated and do not provide physical insight. A simpler, analytical approach is adopted here. It has been observed that "the stress in packed granular materials is concentrated along chains and not distributed uniformly inside the medium" [Liu, Nagel, Schecter, Coppersmith, Majumdar, Narayan, and Witten, 1995]. The measurements from Liu et al. are reproduced in Fig. 1, which shows an image of the force chains as viewed through a cross polarizer. The bead size is shown in red, indicating that the force chains are just a few grains wide.

An idealized representation of force chains is shown in Fig. 2, in which force chains are approximated by sinusoidally varying stress bands. The force chains are assumed to be a few grain diameters in width, which allows the effective medium approximation to be invoked at a local scale.

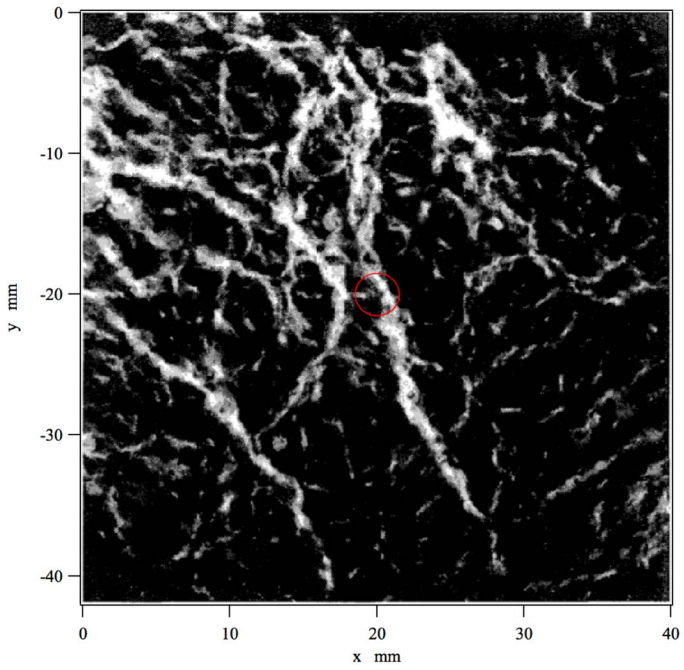

Fig. 1. Force chains in a bead pack, as detected by cross polarizers, from Liu et al. 1995. The image size is 40 mm by 42 mm. The beads are 3 mm pyrex spheres surrounded by an index matching liquid. A 3 mm sphere is drawn in red to show the relative sizes of the force chains and the beads. [The image shows connected force chains in white against a black background. Numerous force chains appear to radiate outward from the top left corner in response to a force applied by a piston from the top.]

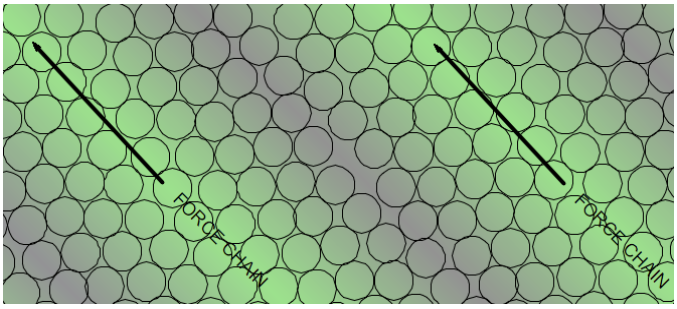

Fig. 2. Idealization of force chains as sinusoidally varying stress bands. [The image shows force chains as stress bands running through close-packed spherical grains.]

This model suggests that the contact stiffness may be approximated as an even sinusoidal function of azimuth angle. In the simplest case, it may be modeled as a contact stiffness that varies sinusoidally about the azimuth dimension of a grain, as illustrated in Fig. 3.

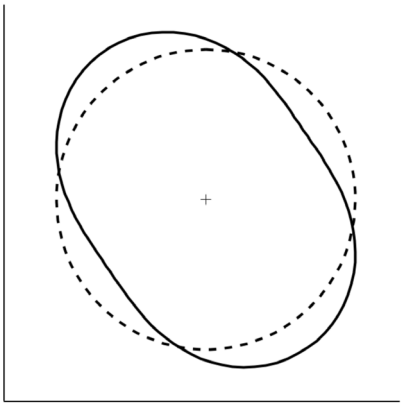

Fig. 3. The average contact stiffness as a function of azimuth angle about a spherical grain (dashed circle) and the azimuthally varying stiffness (solid curve).
[A dashed circle representing the average contact stiffness and a solid oval representing the azimuthally varying stiffness function.]

Using this approximation, the analytical energy equations in Chotiros and Isakson 2011 may be modified to solve the problem of shear and compressional wave speeds in a granular medium with force chains. The work is ongoing.

As a verification exercise, the BIC08 model was fitted to the shear wave attenuation measurements of Brunson [Brunson 1983]. The fit is significantly better than any other model, as shown in Fig. 4. The parameter values needed to obtain a good fit to the attenuation data are shown in Table I. Physical inconsistencies arose when the model was used to compute the physical dimensions, particularly the fluid film width and thickness at the grain-grain contact.

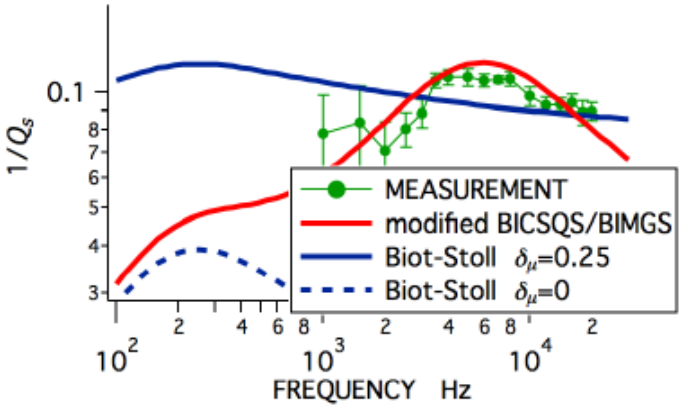

Fig. 4. Measurement of shear speed attenuation, in terms of 1/Q, as a function of frequency (green) from Brunson 1983 compared to the Biot-Stoll model, with and without a shear log decrement (blue solid, blue dashed), and the modified BICSQS/BINGS, aka BIC08 (red).
[Measurement of shear speed attenuation by Brunson 1983 shows a strong frequency dependence, particularly a peak near 10 kHz. It is well matched by the BICSQS/BIMGS model.]

Table I. Parameter values of the BIC08 model in SI units

Parameter	Value
ρ_s Grain density (tables)	2650
k_r Grain bulk mod. (tables)	36E9
ρ_f Fluid density (tables)	1000
k_f Fluid bulk mod. (tables)	2E9
β Porosity (meas.)	0.355
η Viscosity (tables)	0.001
κ Permeability (meas.)	1.1E-10
a_p Pore size (calc./meas.)	7E-5
c Tortuosity (calc./meas.)	1.65
K_b Frame bulk mod(fit speed)	5.7E7
K_y Frame bulk inc. (fit)	8.6E7
f_k Bulk relax. Freq. (fit)	1800
$f_{\square}$Shear relax. Freq. (calc.)	1E7

The dimensions of the fluid film at the grain-grain contact may be estimated, using the equations derived by Kimura [Kimura 2006],

$$f_k = \frac{k_f}{12\eta}\left(\frac{h}{a}\right)^2 \qquad (1), \quad \text{and} \quad K_y = \frac{a^2 k_f}{h}\frac{n(1-\beta)}{12R_g} \qquad (2)$$

where a and h are the radius and thickness of the fluid film, R_g the grain radius (=0.2 mm) and n the coordination number (=9 approx.). Solving for a and h, using parameter values in the table, the answers obtained are 8.2E-9 and 1.7E-12 m, respectively. The last value is clearly unphysical, because the film thickness cannot be less then the diameter of a molecule of water, which is 3E-10 m. It would be unphysical to have a film of water that is a hundred times thinner than a water molecule. The solution to this inconsistency was found in recently reported measurements in the field of micro-fluidics. Measurements with an atomic microscope show that the viscosity of water between hydrophilic surfaces (silica) changes dramatically when the gap thickness is reduced to a few nano-meters [Goertz et al. 2007, Riedo 2007]. From the measurements of Goertz et al., the viscosity as a function of film thickness was estimated, as shown in Fig. 5. Equations (1) and (2) may also be inverted to give an expression of viscosity η as a function of film thickness h, also plotted in Fig. 5.

$$\eta = \frac{hk_f^2 n(1-\beta)}{144 K_y f_k R_g} \qquad (3)$$

The intersection of the two curves gives a physically plausible solution for the film thickness, which is approximately 2 nm, or about seven water molecule diameters. This solution shows that micro-fluidic effects need to be taken into account, and it opens the way to a more robust model with a reduced number of input parameters.

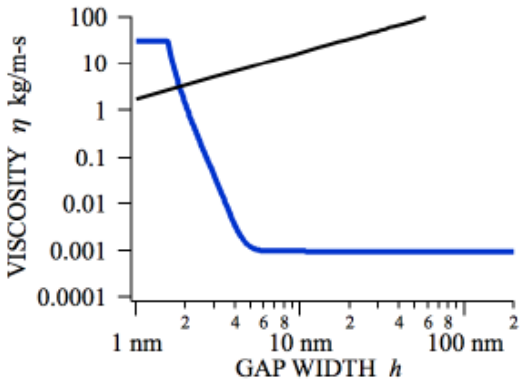

Fig. 5. Estimated viscosity of a water film confined between hydrophilic surfaces as a function of film thickness (blue) based on Goertz et al. 2007. The intersection of this curve with the curve of viscosity vs film thickness (black) from equation (3) gives a solution for the film thickness. [Estimated viscosity of water shows an increase of 6 orders of magnitude as the film thickness drops below 5 nanometers.]

(2) A new model of sediment reflection: Transmission loss (TL) data from a measurement exercise was analyzed to investigate possible causes of TL uncertainty. Two TL measurement tracks over a sandy seabed that were practically identical, but displaced by a few kilometers, were compared, as illustrated in Fig. 6.

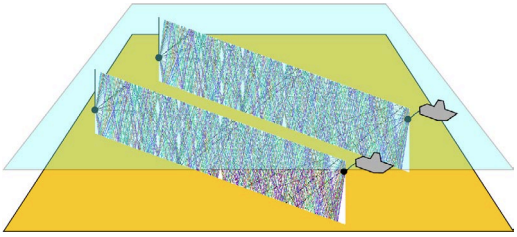

Fig. 6. Illustration of two TL tracks displaced by a few kilometers. [The illustration shows a receiving array and a towed sound source along two parallel tracks.]

The differences in TL, as a function of range and frequency were measured, for the ranges up to 10 km and for the frequency band 60 to 320 Hz. A model of the TL variations was constructed, using all the environmental data collected during the measurements, including surface motion, sound speed profile variations and bottom properties. By comparing the modeled and measured RMS TL differences between the two tracks, as shown in Fig. 7, it was determined that the main cause of TL fluctuations was the patchiness of the bottom properties.

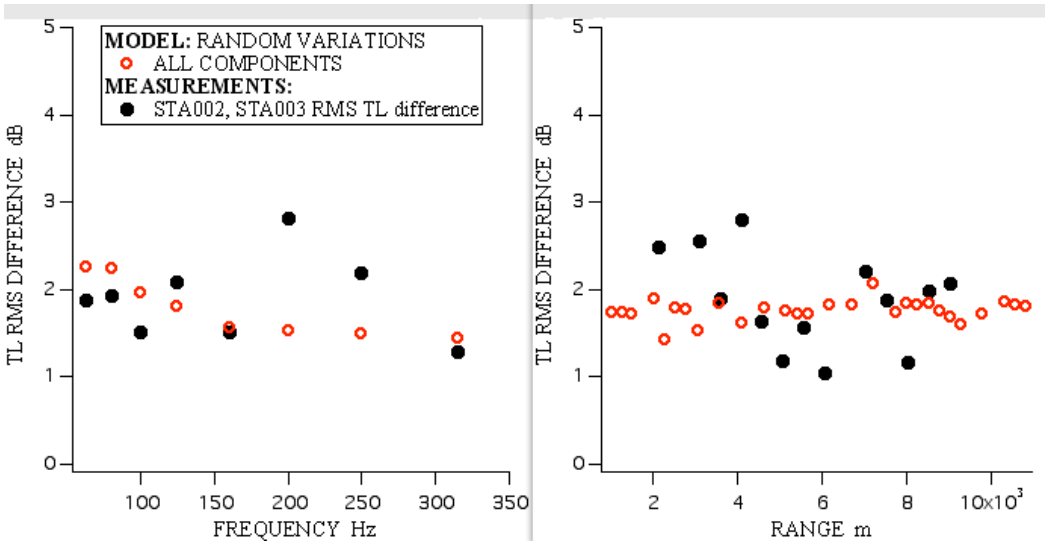

Fig. 7. Measured (black circles) and modeled (red cirlces) RMS TL differences as a function of frequency (left) and range (right) between the two tracks.
[The graphs show approximate agreement between the measured (black circles) and modeled (red circles) RMS TL differences.]

(3) Coupling of BIC08 to rough surface scattering models: The approach is to replace the poro-elastic medium half-space with a thin poro-elastic layer overlaid on a fluid half-space of the same density and compressional wave speed, which in turn may be terminated by a perfectly matched layer (PML). To illustrate the problem, the transmission loss in a simple waveguide was investigated. The waveguide consists of water over a sandy bottom modeled as an elastic half-space, which serves as a proxy for the poro-elastic medium, as shown in Fig. 8. In this example, the elastic half space has a density of 2073 kg/m^3, and wave speeds compressional 1708 and shear 123 m/s, respectively. The wave attenuations are 1.47 and 1.76 dB per wavelength, respectively. The water has a density 1023 kg/m^3 and wave speed 1523 m/s. These parameter values are typical of the West Florida sand sheet. The source and receiver are at a depth of 4 m, and the frequency was set at 1 kHz. OASES was used to make the transmission loss (TL) calculations. This problem is difficult for FEM because the relatively slow shear wave causes the mesh density in the bottom halfspace to be very high. By modeling the bottom as a thin layer of elastic material over a fluid material of the same density and longitudinal wave speed, as shown in Fig. 9 the high mesh density region is minimized and the problem becomes manageable.

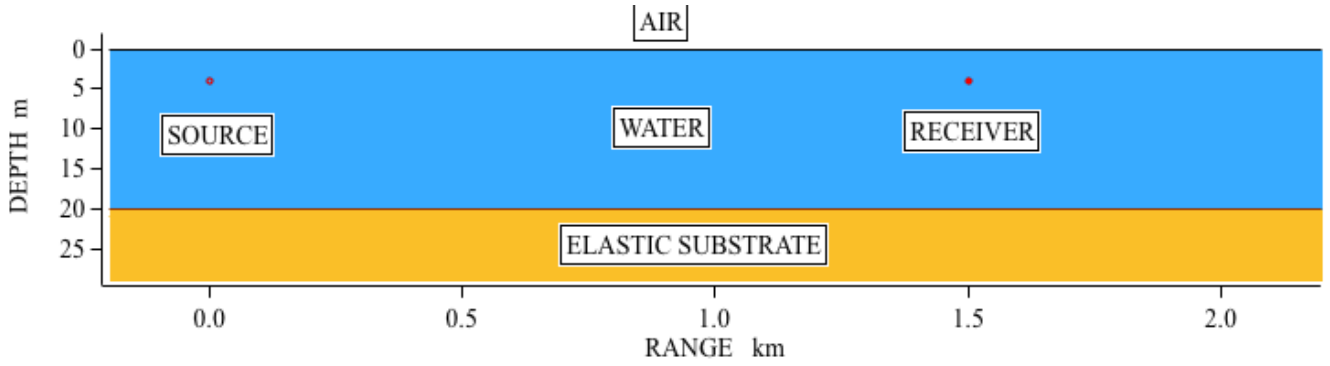

Fig. 8. Model of a shallow water wave guide with iso-speed water 20 m deep, over an elastic seabed, with source and receiver at a depth of 4m.
[Illustration of a shallow water waveguide, with water in blue and seabed in brown, and red dots marking source and receiver positions.]

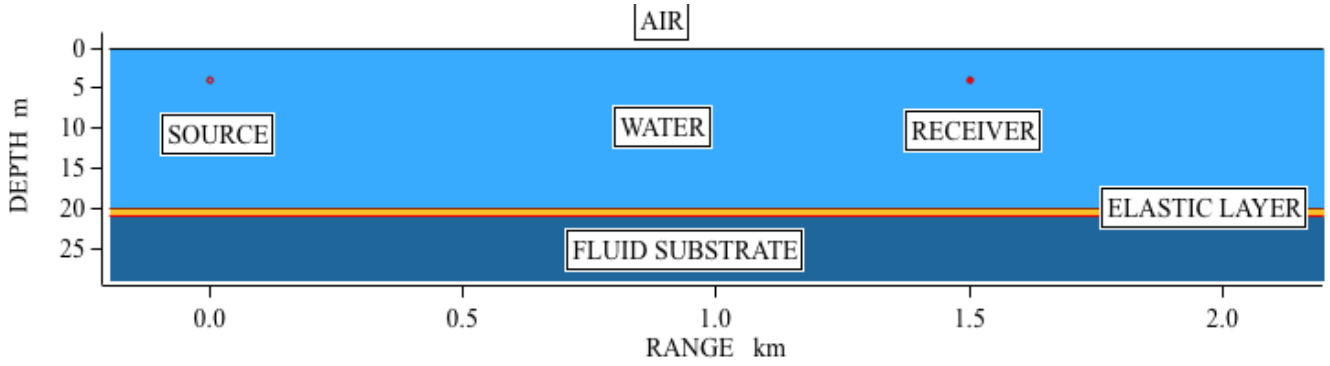

Fig. 9. Model of a shallow water wave guide with iso-speed water 20 m deep, over a thin elastic layer and a fluid seabed of the same sound speed and density, with source and receiver dashed at a depth of 4m.
[Illustration of a shallow water waveguide, with water in blue, elastic layer in brown, fluid seabed in a darker blue, and red dots marking source and receiver positions.]

The results for a number of layer thicknesses are shown: 0.0, 0.1, 0.3 and 0.1 m. The TL curves are shown in Fig. 10. The TL difference between the half-space model and the layered models are shown in Fig. 11. The largest TL differences appear to occur in the nulls. For zero layer thickness, differences up to 3 dB are observed. The TL difference decreases as the layer thickness is increased. At a layer thickness of 1 m, the TL difference is reduced to less than half a decibel, indicating that this approach may be viable.

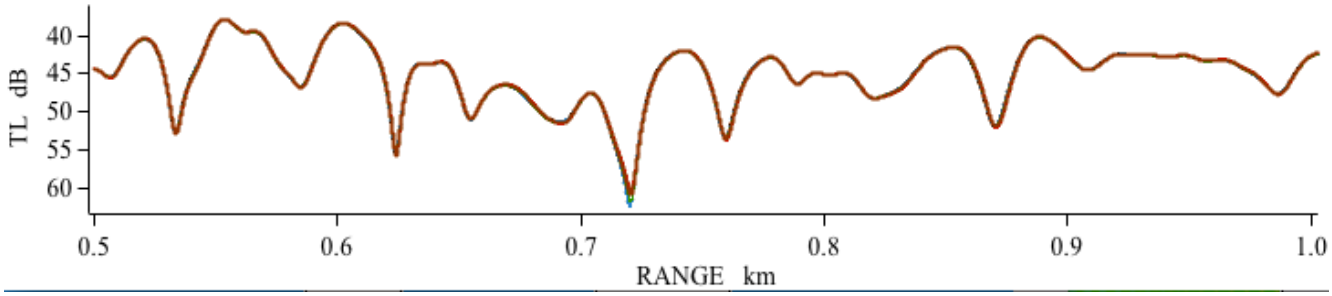

Fig. 10. Computed transmission loss (TL) as a function of range between source and receiver for all models.
[The TL plot shows variations of about 20 dB. The different models agree within a few dB.]

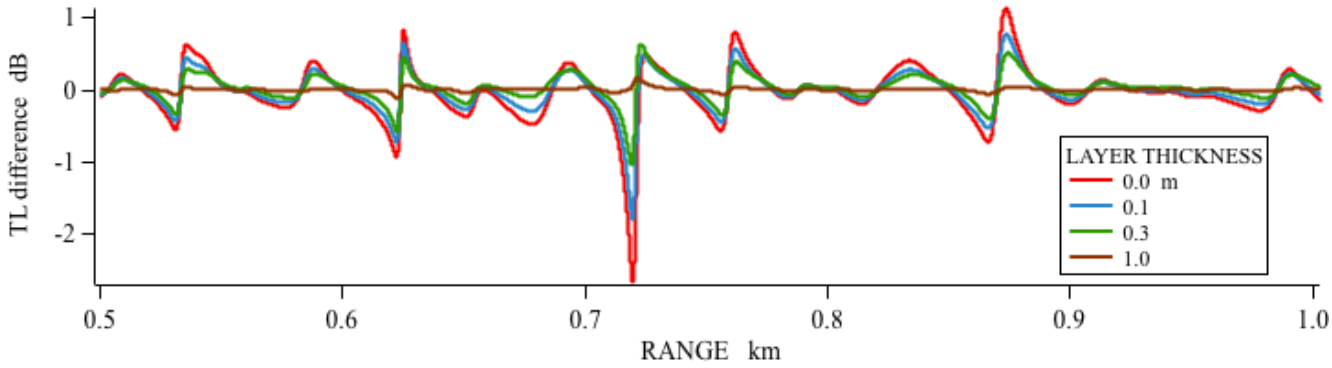

Fig. 11. Differences in TL between the elastic seabed model and the models that employ an elastic layer over a fluid seabed.
[Differences of up to 3 dB are shown. The 1 m layer thickness gave the smallest differences. The curves are color coded for different layer thicknesses: 0 red, 0.1 blue, 0.3 green, 1.0 brown.]

It is also instructive to look at the corresponding bottom reflection coefficients. The difference between the reflection coefficient of the layered models to the elastic half space model is shown in Fig. 12. Even though the reflection loss differences are very small, less than 0.1 dB, the multiplicity of bottom interactions causes an accumulation that leads to TL differences of several decibels. It is also noticed that, at a layer thickness of 1 m, the reflection loss difference at angles below critical, which is approximately 30 degrees, is practically zero. This is the angle range that is most critical to long range propagation.

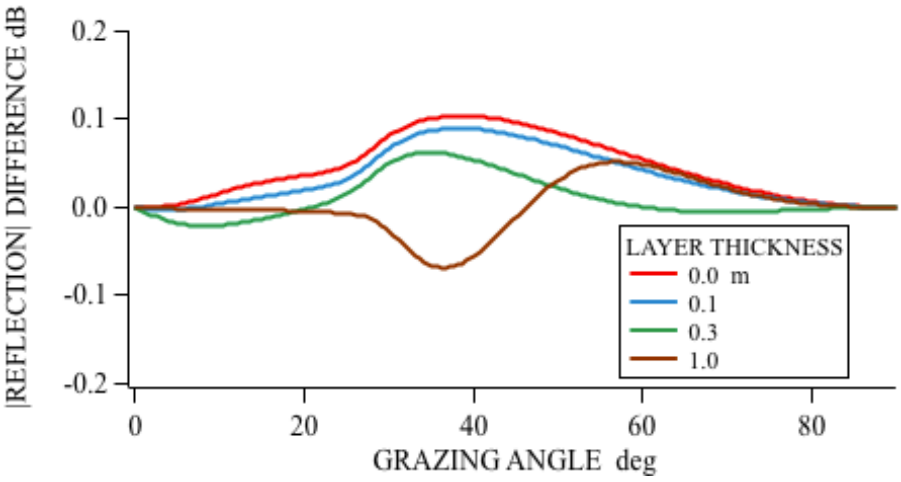

Fig. 12. Differences between the reflection magnitudes of the water-elastic seabed interface and the water-elastic layer-fluid seabed models, with different layer thicknesses. [The curves are color coded to correspond with the TL difference curves. The differences are between + and – 0.1 dB.]

IMPACT/APPLICATIONS

The results will impact Navy underwater acoustic propagation models, particularly where reflection and penetration of sound at the ocean bottom are concerned. It will also impact the future structure of oceanographic databases maintained by Navy offices, including the Naval Oceanographic Office. Predictions of sediment wave speeds and attenuations will need to be revised.

TRANSITIONS

Work on sediment variability is being transitioned to the active sonar trainers via the High-Fidelity Active Sonar Training (HiFAST) project and to future projects to improve the HFBL database. Some aspects of the ocean sediment model, particularly the frequency dependence of sediment attenuation, are being used in the Ocean Bottom Characterization Initiative (OBCI) project.

RELATED PROJECTS

This project is closely related to most projects under the ONR Underwater Acoustics: High Frequency Sediment Acoustics and Shallow Water Thrusts.

REFERENCES

B. A. Brunson. "Shear wave attenuation in unconsolidated laboratory sediments," Ph. D. Corvalis, (1983)

N. P. Chotiros and M. J. Isakson, "A broadband model of sandy ocean sediments: Biot-Stoll with contact squirt flow and shear drag," *J. Acoust. Soc. Am*., vol. 116, pp. 2011-2022, (2004).

N. P. Chotiros and M. J. Isakson, "Acoustic virtual mass of granular media," J. *Acoust. Soc. Am.*, vol. 121, pp. EL70-EL76, (2007).

N. P. Chotiros and M. J. Isakson, "High-frequency dispersion from viscous drag at the grain-grain contact in water-saturated sand," *J. Acoust. Soc. Am.*, vol. 124, pp. EL296-301, (2008).

N. P. Chotiros, and M. J. Isakson. "Shear and compressional wave speeds in Hertzian granular media," J. Acoust. Soc. Am. **129**, 3531-3543, (2011).

M. J. Isakson, N. P. Chotiros, H. J. Camin, and J. Piper. "Bottom Loss Measurements in a Spatially Variable Environment at the Sediment Acoustics Experiment 2004," J. Acoust. Soc. Am., (2010)

M. P. Goertz, J. E. Houston, and X.-Y. Zhu, "Hydrophilicity and the Viscosity of Interfacial Water," *Langmuir*, vol. 23, pp. 5491-5497, (2007).

M. Kimura. "Frame bulk modulus of porous granular marine sediments," J. Acoust. Soc. Am. 120, 699-710, (2006).

B. J. Kraft and C. P. de Moustier, "Detailed Bathymetric Surveys Offshore Santa Rosa Island, FL: Before and After Hurricane Ivan (September 16, 2004)," *IEEE J. Oceanic Eng.*, vol. 35, pp. 453-470, (2010).

C. H. Liu, S. R. Nagel, D. A. Schecter, S. N. Coppersmith, S. Majumdar, O. Narayan, and T. A. Witten. "Force fluctuations in bead packs," Science 269, 513-515, (1995)

A. P. Lyons and D. A. Abraham, "Statistical characterization of high-frequency shallow-water seafloor backscatter," *J. Acoust. Soc. Am.*, vol. 106, pp. 1307-1315, (1999).

L. La Ragione, and J. T. Jenkins. "The initial response of an idealized granular material," Proc. R. Soc. London, Ser. A 463 735-758, (2007)

E. Riedo. "Water behaves like a viscous fluid on the nano-scale," Membrane Technology August 2007, 8, (2007)

J. T. Jenkins, D. L. Johnson, L. La Ragione, and H. A. Makse. "Fluctuations and the effective moduli of an isotropic, random aggregate of identical, frictionless spheres," J. Mech. Phys. Sol. 53, 197-225, (2005)

PUBLICATIONS

1. N. P. Chotiros, and M. J. Isakson. "Shear and compressional wave speeds in Hertzian granular media," J. Acoust. Soc. Am. 129, 3531-3543, (2011).
2. M. J. Isakson, and N. P. Chotiros. "Finite element modeling of reverberation and transmission loss in shallow water waveguides with rough boundaries," J. Acoust. Soc. Am. 129, 1273-1279, (2011)

3. K. R. Loeffler, and N. P. Chotiros. "The Calibration of a Laser Profiling System for Seafloor Micro-topography Measurements," International Journal of Ocean Systems Engineering, accepted (2011)

4. N. P. Chotiros, and M. J. Isakson. "Shear wave attenuation in underwater granular media," J. Acoust. Soc. Am. 4 pt. 2, 2358, (2010)

5. M. J. Isakson, and N. P. Chotiros (2011). "Reverberation Statistics for HiFAST," in FNC Review of HIFAST for Sonar Operators (NRL, DC, USA).

6. N. P. Chotiros (2011). "Sediment acoustics: Wideband model, reflection loss and ambient noise inversion " in ONR OA FY11 Peer Review (NRL Stennis Space Station, MS, USA).

7. N. P. Chotiros, and M. J. Isakson. "Compressional and shear wave modeling in underwater granular media," J. Acoust. Soc. Am. 129, 2389-2390, (2011).

8. M. J. Isakson, and N. P. Chotiros (2011). "ARL:UT Plan for Reverberation Field Experiment: Reflection and forward scatter," in Reverberation Field Experiment Workshop (DC, USA).

9. N. P. Chotiros (2011). "Seafloor properties for practical applications," in Underwater Defense Technology 2011 Conference (London, UK).

10. N. P. Chotiros. "High frequency bottom backscattering strength at shallow grazing angles," Underwater Acoustic Measurements: Technologies and Results, 4th International Conference, Kos, Greece, 20-24 June 2011, 1699-1676, (2011)

11. M. J. Isakson, and N. P. Chotiros. "Modeling the effects of boundary roughness on transmission loss measurements in shallow water waveguides using finite elements," Underwater Acoustic Measurements: Technologies and Results, 4th International Conference, Kos, Greece, 20-24 June 2011, 29-36, (2011)

12. M. J. Isakson, N. P. Chotiros, and S. Joshi (2011). "Interface Scattering and Layering Effects in Transmission Loss Variability," in HFBL Variability Meeting (Solana Beach, CA, USA).

13. N. P. Chotiros, and M. J. Isakson (2011). "Ambiguity and variability of bottom loss inverted from TL measurements," in HFBL Variability Meeting (Solana Beach, CA, USA).